Ultrasonics 51 (2011) 115–122

Contents lists available at ScienceDirect

Ultrasonics

journal homepage: www.elsevier.com/locate/ultras

Dependence of optimal seed bubble size on pressure amplitude at therapeutic pressure levels

Kelsey J. Carvell [a], Timothy A. Bigelow [b,*]

[a] Department of Electrical and Computer Engineering, Iowa State University, Ames, IA 50011, USA
[b] Department of Electrical and Computer Engineering and Department of Mechanical Engineering, Iowa State University, Ames, IA 50011, USA

ARTICLE INFO

Article history:
Received 7 April 2010
Received in revised form 22 June 2010
Accepted 28 June 2010
Available online 15 July 2010

Keywords:
Cavitation
Optimal bubble size
Ultrasound therapy

ABSTRACT

Medical ultrasound has shown great potential as a minimally invasive therapy technique. It can be used in areas such as histotripsy, thermal ablation, and administering medication. The success of these therapies is improved by the cavitation of small microbubbles, and often it is useful to know which bubbles might provide the most effective therapy. When using therapies based on stable cavitation, the optimal bubble size is approximately given by $R_0 \cong 3$ MHz μm$/f_0^{lin}$. However, a similar expression is not available for therapies involving inertial cavitation. Therefore, the goal of our study was to develop an approximate expression relating the initial size of the bubble that resulted in the maximum response to the ultrasound operating frequency and pressure of the ultrasound wave when inertial cavitation is expected. The study was conducted by simulating the response of air bubbles in water to linearly propagating sine waves using the Gilmore–Akulichev formulation to solve for the bubble response. The frequency of the sine wave varied from 0.5 to 5 MHz while the amplitude of the sine wave varied from 0.0001 to 5 MPa. The optimal initial size for a particular frequency of excitation and amplitude, which is normally only established for stable cavitation, was defined in the study as the initial bubble size that resulted in the maximum bubble expansion prior to bubble radius dropping below its initial radius. A fit over pressure and frequency then yielded that the optimal size was approximately given by $R_{optimal} = (0.0327f^2 + 0.0679f + 16.5P^2)^{-0.5}$ where $R_{optimal}$ is in μm, f is the frequency of the ultrasound wave in MHz, and P the pressure amplitude of the ultrasound wave in MPa.

1. Introduction

For years ultrasound has shown remarkable potential as a tool for minimally invasive therapy. Most procedures use the energy in the ultrasound waves to heat and kill targeted tissue [1–5]. In addition to killing tissue, ultrasound therapies are being successfully developed to enhance thrombolysis [6], improve drug and gene delivery [7,8] control bleeding and hemorrhaging from severe trauma [9,10], erode or liquefy tissue [1,11,12], and destroy bacteria biofilms [13]. Many of these developing therapies have been found to depend upon or be significantly enhanced by the cavitation of microbubbles. Cavitation is the response of gas bubbles in liquid after oscillating to an acoustic field. There are two specific types; stable and inertial cavitation. Stable cavitation is the relatively small oscillations (less than a few percent) of the bubble's radius about its equilibrium radius. These oscillations may generate microstreaming in the vicinity of the bubble leading to improved sonoporation [14–19], but otherwise have no observable effect on the tissue. The amplitude of the oscillations during stable cavitation experiences a resonance that depends on the size of the bubble and frequency of the sound. When a bubble is driven at its resonance frequency during stable cavitation it reaches higher oscillation amplitudes and will provide more effective therapy.

The traditional relationship between resonance frequency, f_0^{lin}, and resonance size, R_0, for low level acoustic excitations pertinent to stable cavitation is given by

$$f_0^{lin} = \frac{1}{2\pi R_0\sqrt{\rho_o}}\sqrt{3\eta\left(P_o + \frac{2\sigma}{R_0} - P_v\right) - \frac{2\sigma}{R_0} - \frac{4\mu^2}{\rho_o R_0^2}} \quad (1)$$

where P_o is the ambient pressure of the liquid, σ is the surface tension of the bubble, ρ_o is the equilibrium liquid density of the fluid, η is the polytropic exponent, P_v is the vapor pressure inside of the bubble, μ is the coefficient of shear viscosity for the fluid, and R_0 is the initial bubble radius [20–23]. This equation was derived by a linearization of the Keller–Herring model for bubble dynamics shown in MacDonald et al. [20]. The derivation assumes that the pressure amplitude of the incoming sine wave to be much smaller than the ambient static pressure, which would correlate to

* Corresponding author. Address: Department of Electrical and Computer Engineering, Iowa State University, 2113 Coover Hall, Ames, IA 50011, USA. Tel.: +1 515 294 4177; fax: +1 515 294 3637.
E-mail address: bigelow@iastate.edu (T.A. Bigelow).

0041-624X/$ - see front matter © 2010 Elsevier B.V. All rights reserved.
doi:10.1016/j.ultras.2010.06.005

pressures which result in stable cavitation oscillations. The expression in Eq. (1) is often simplified by neglecting surface tension and viscosity and assuming an air bubble in water to yield [24,25]

$$R_0 \cong 3\ \text{MHz}\ \mu\text{m}/f_0^{lin}. \quad (2)$$

Eq. (2) is often useful in determining the approximate bubble sizes of interest when designing an ultrasound therapy experiment. For example, if one is operating at 1 MHz, then bubbles on the order of 3 μm are needed in the ultrasound field. If a better understanding of the bubble/cell interactions is needed, then detailed computer models may be necessary but Eq. (2) provides a convenient place to start when working with stable cavitation.

Inertial cavitation is the dramatic expansion and violent collapse of the gas bubble that occurs at higher acoustic pressure levels (greater than ~1 MPa with a dependence on frequency and bubble size) and is more complicated than stable cavitation. In therapy applications, inertial cavitation is used most commonly to mechanically destroy cells or tissue in histotripsy, tissue erosion, or similar applications [1,11–13]. During inertial cavitation the bubble expands to many times its original size and collapses violently causing microjets that can shred tissue. This process occurs over a small number of acoustic cycles, usually three or less, before the collapse takes place. Therefore, it is more difficult to determine the resonance size/frequency for a bubble undergoing inertial cavitation because numerous acoustic cycles cannot be used to remove the impact of other transients in the dynamic system. However, there is still an optimal initial bubble size ("seed" size) which results in the most dramatic bubble response for a particular ultrasound exposure. However, unlike for stable cavitation, during inertial cavitation the optimal seed size exhibits a strong dependence on pressure amplitude [20]. Therefore, (2) is not valid for obtaining approximate estimates when planning ultrasound therapy procedures involving inertial cavitation. Hence, there is a need for an approximate expression, similar to (2), that would be useful when designing or understanding ultrasound therapy applications involving inertial cavitation.

The goal of our study was to develop an approximate expression relating the optimal initial "seed" size of the bubble to the ultrasound operating frequency and pressure of the ultrasound wave when inertial cavitation is expected which could be used similar to (2) for therapy planning. To this end, the response of a spherically symmetric air bubble in an unbounded water media to ultrasound waves was simulated. An air bubble in water was selected as this was the simplest model for inertial behavior and would be analogous to the air bubble in water used when deriving (2). Since we were interested in the optimal bubble size/frequency relationship for a bubble undergoing inertial cavitation, a stabilizing shell as is found on ultrasound contrast agents was not included since this shell would rupture releasing a "free" bubble after the first ultrasound pulse [26]. Furthermore, we are primarily interested in inertial cavitation applications, such as histotripsy, where encapsulated bubbles would not be present. Our work is similar to the studies of inertial cavitation previously conducted by Church et al. [27–30], however their work did not focus on finding an empirical relationship between optimal bubble size and excitation frequency.

In our study, we solved the Gilmore–Akulichev formulation for bubble dynamics to find the optimal seed size at different frequencies as a function of excitation amplitude. For the purposes of this study, the optimal seed size was defined as the initial bubble size that results in the greatest bubble expansion relative to the initial size prior to the bubble radius falling below the initial radius (i.e., first collapse). The simulations found the optimal seed size for pressure amplitudes of 100 Pa–5 MPa for acoustic frequencies of 1, 3, and 5 MHz. Previously, other investigators have shown a decrease in resonance size with increasing pressure [20,22], but they only considered pressures on the order of 1 MPa or less, well below the acoustic pressures used to induce inertial cavitation in many biomedical applications. After finding the optimal seed size for each ultrasound exposure condition, a curve was fit to all of the data to obtain an approximate analytical expression.

2. Description of simulation parameters

2.1. Equations solved

In our study, the Gilmore–Akulichev formulation for bubble dynamics was used to simulate the bubble. This formulation was selected given its prevalence when studying cavitation collapse at high pressure levels [27–30]. Also, the Gilmore–Akulichev formulation is capable of calculating the response of a bubble at higher acoustic pressures (prior to bubble fragmentation) without requiring the complexity and computational cost of three-dimensional models of bubble dynamics. Viscous and acoustic damping, which are the primary damping factors for the frequencies and bubble sizes of interest in our study [28], were included by Eqs. (2)–(6) as has been done previously [27,28]. Other models such as Rayleigh–Plesset or Keller–Herring, while popular with simulating bubble dynamics for contrast agent and some drug delivery studies [20,31–36], are not valid when the bubble expands more than several times its initial radius [37,38]. In addition, three-dimensional models are not required since the bubble is oscillating in isolation in an unbounded fluid (symmetric collapse), and we are only interested in bubble behavior prior to the inertial collapse when bubble fragmentation is likely. One potential short coming of the Gilmore–Akulichev formulation utilized in this paper was that it did not include heat or mass transfer. Furthermore, the formulation did not include bubble to bubble interaction which impact resonance behavior [39,40]. However, it should still give an approximate response of the bubble sufficiently accurate to develop a reasonable analytical expression relating optimal seed size to pressure and frequency.

To further simplify our analysis, we assumed that the ultrasound waves were not corrupted by nonlinear propagation distortion so that the acoustic excitation only had a single frequency (i.e., no harmonics or sub-harmonics). While this approximation would not be valid for real ultrasound fields, it was necessary to simplify the problem at this stage. Waveform distortion introduced by nonlinear propagation depends strongly on the focusing properties of the source. Therefore, in order to include nonlinear propagation, multiple focusing schemes would need to be included in the analysis. The inclusion of source focusing would likely make our analytical expression relating optimal seed size to pressure and frequency too cumbersome to be used in first order calculations. In order to minimize the impact of neglecting nonlinear propagation, we chose to focus on the maximum bubble expansion prior to the initial collapse in our study which would be most dependent on the rarefactional pressure. The rarefactional portion of the wave is not impacted as much as the compressional portion of the wave by nonlinear propagation.

The Gilmore–Akulichev formulation for bubble dynamics is given by

$$R\left(1-\frac{U}{C}\right)\frac{dU}{dt}+\frac{3}{2}\left(1-\frac{U}{3C}\right)U^2=\left(1-\frac{U}{C}\right)H+\frac{U}{C}\left(1-\frac{U}{C}\right)R\frac{dH}{dR} \quad (3)$$

Eq. (3) represents the response of a single bubble with respect to time. The R corresponds to the radius of the bubble, and U is the bubble wall velocity (i.e., $U = dR/dt$). The other parameters are given by

$$C = \left[C_0^2 + (m-1)H\right]^{1/2} \tag{4}$$

$$H = \int_{P_\infty}^{P(R)} \frac{dP}{\rho} \tag{5}$$

where C is the speed of sound at the bubble wall and is calculated from the infinitesimal speed of sound in the liquid, C_0 set to 1500 m/s, a constant m normally set to seven as is explained in [41], and the enthalpy of the liquid, H. The enthalpy is related to the pressure in the fluid far from the bubble, P_∞, and the pressure at the bubble wall, $P(R)$. These pressures are given by

$$P_\infty = P_o - p_{acoustic} \tag{6}$$

$$P(R) = P_g - \frac{2\sigma}{R} - \left(\frac{4\mu}{R}\right)U \tag{7}$$

where P_o is the ambient pressure of the liquid, $p_{acoustic}$ is the pressure associated with the acoustic wave, σ is the surface tension of the bubble wall set to 6.8 Pa cm (in the range of measure surface tension for an air/water interface), and μ is the coefficient of shear viscosity set to 0.001 Pa s as has been measured for water. P_g is the total pressure of the gas inside the bubble and is given by

$$P_g = \left(P_o + \frac{2\sigma}{R_0} - P_v\right)\left(\frac{R_0}{R}\right)^{3\eta} + P_v \tag{8}$$

where R_0 is the equilibrium radius set equal to the initial radius for our simulations, P_v is the vapor pressure inside the bubble at the equilibrium radius, and η is the polytropic exponent initially set to 1.4 for our study. The polytropic exponent governs the thermodynamic behavior of the gas in the bubble. If the gas is assumed to be adiabatic, as was done in our study, than it is the ratio of the specific heats (i.e., specific heat at constant pressure over specific heat at constant volume). Similarly, for isothermal processes, the polytropic exponent would be set to 1. In addition, the time varying pressure is related to the time varying density of the liquid, ρ, by

$$P = \alpha(\rho/\rho_o)^m - \beta \tag{9}$$

where ρ_o is the equilibrium liquid density of the fluid, set to 1000 kg/m^3, while α and β are constants describing the fluid. The constants of α and β are defined as follows; $\alpha = C_i^2\rho/P_o m$ and $\beta = \alpha - 1$.

The simulations in this study involved an air bubble in water. The simulations found the optimal seed size for pressure amplitudes of 100 Pa–5 MPa for acoustic frequencies of 1, 3, and 5 MHz. These pressures and frequencies were selected based on their relevance to therapeutic ultrasound. A function in MATLAB (The MathWorks Inc., Natick, MA) was written to scan initial bubble sizes searching for the maximum expansion relative to the initial size, prior to when the bubble dropped below its initial size. Finding this optimal seed size was the primary goal of the simulations. Our optimal seed size was also used to find the maximum expansion of the bubble relative to the initial size over 50 acoustic cycles or until the initial radius dropped below one tenth its initial size (neglecting bubble fragmentation and assuming rebound).

2.2. Justification for new definition of optimal seed size

The traditional definition of resonance size stems from a relationship between the frequency of the acoustic waves and the bubble radius in the acoustic field. A bubble at the resonance size for a particular frequency would undergo maximum changes to its radius when excited at that frequency once any transient behavior of the dynamic system has subsided. The oscillations for bubbles of a different size would be less than the oscillations at the resonance size. The traditional relationship between resonance frequency and resonance size for low level acoustic excitations is given by (1) [20,21]. This equation was derived by a linearization of the Keller–Herring model for bubble dynamics shown in MacDonald et al. [20] as was mentioned in the introduction. The linearization of the Keller–Herring shown in (1) is given as a reference for microbubble resonance and is not derived from the Gilmore–Akulichev formulation.

While the traditional definition of resonance size, given by (1), works well for stable cavitation applications, it is impossible to define when inertial cavitation is present. When undergoing inertial cavitation a single bubble would typically undergo one expansion prior to a violent collapse, which would leave the bubble in fragments. Furthermore, even if the bubble did not fragment and the bubble radius rebounded for many cycles, the response of the bubble would not be periodic as is illustrated in Fig. 1. Fig. 1a shows a bubble undergoing stable cavitation while Fig. 1b shows a bubble undergoing inertial cavitation and rebound as simulated in our study. The transient behavior in Fig. 1a passes after about 5–10 acoustic cycles leaving a periodic sinusoidal oscillation while the oscillations in Fig. 1b never exhibit any periodicity even out to 50 acoustic cycles. Therefore, it is impossible to "wait" until the transient behavior of the system has subsided when determining a resonance size/frequency for a bubble undergoing inertial cavitation. For this reason, a modified definition of optimal size was used in our study.

When determining an optimal size for inertial cavitation, we defined the optimal seed size for a particular acoustic frequency as the initial bubble size that resulted in the largest bubble expansion prior to when the size of the bubble dropped below its initial size (i.e., first collapse). This definition avoids the complication of bubble fragmentation that would alter the bubble size while still providing some guidance to inertial cavitation based therapies. For consistency, this definition was used throughout the entire range of pressure amplitudes rather than just for amplitudes where inertial cavitation was expected. While quantifying bubble collapse velocity might be a more intuitive method for quantifying cavitation, we chose to focus on the bubble expansion because it would be easier to validate our results experimentally using a high speed camera system if we focused on the maximum expansion. Further-

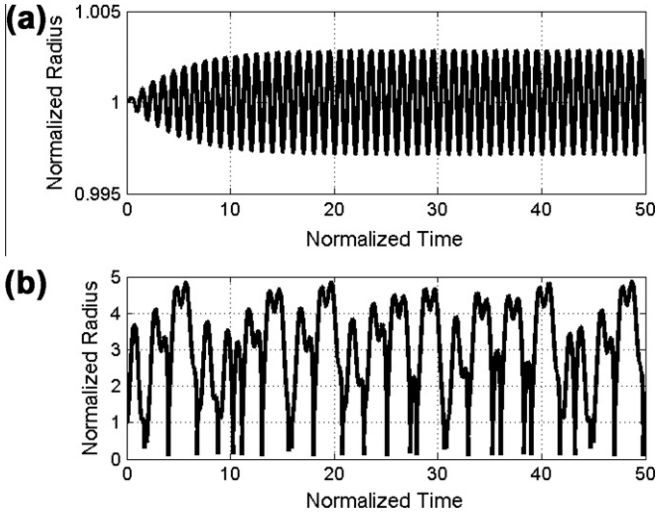

Fig. 1. An example bubble with an initial radius of 3.704 μm undergoing: (a) stable cavitation and (b) inertial cavitation. For stable cavitation, the simulated bubble was driven at 1 MHz and 100 Pa while for inertial cavitation the simulated bubble was driven at the same frequency, 1 MHz but with a higher pressure amplitude, 1 MPa. Both plots show the radius normalized to the initial radius and the time normalized to the acoustic period.

Table 1
Comparisons between the traditional definition of resonance size and our new definition of optimal seed size developed to study the relationship between bubble size and frequency at higher pressure amplitudes.

Frequency	0.5 MHz	1 MHz	3 MHz	5 MHz
Traditional/theoretical resonance radius	*6.95* μm	*3.67* μm	*1.42* μm	*0.94* μm
New optimal seed radius found in simulations	5.20 μm	2.99 μm	1.42 μm	0.94 μm

more, preliminary simulation results also demonstrated that the two were equivalent. Our new definition for optimal seed size does not generally give the same size as the traditional definition for resonance size even for smaller excitation pressures inducing stable bubble oscillations as is illustrated by Table 1.

Table 1 shows both the traditional/theoretical resonance size and the new optimal seed size found under our new definition. The traditional size was found from (1) while the new size was found via computer simulations for a pressure amplitude of 100 Pa. The new optimal seed size is approximately the same as the traditional size for 3 and 5 MHz, but is clearly different at the lower frequencies (0.5 and 1 MHz). This difference can be attributed to variations in the transient behavior of the microbubble system as is illustrated in Fig. 2. Fig. 2a and b for the 0.5 MHz and 1 MHz cases, show that within the initial cycle the simulated optimal seed size has a slightly larger peak value than the traditional resonance size. After the transients subside, however, the peaks level out smaller than the peaks for the theoretical resonance size bubbles. The peaks for the theoretical resonance size continue to increase until reaching steady state with peaks approximately five times greater than the peaks associated with the new optimal seed size bubbles. However, in Fig. 2c and d corresponding to the 3 and 5 MHz excitation, the curves overlap.

3. Results

3.1. Optimal seed size as a function of pressure and frequency

The dependence of optimal seed size as a function of pressure amplitude is shown in Fig. 3a. It is clear from this figure that with increasing pressure amplitude there will be a reduction in the optimal seed size. Fig. 3b also shows the maximum expansion relative to the initial size when the simulations are allowed to continue over 50 cycles or until the initial size dropped below one tenth its initial size. The maximum expansion of the bubbles also appears to increase dramatically as the optimal seed size of the bubble decreases. Therefore, the drop in optimal size probably correlates with the onset of inertial cavitation as will be discussed later. Another observation of the bubble activity at high pressure amplitudes was the reduced dependence of optimal bubble size on frequency. At low pressure amplitudes (<0.1 MPa) the optimal seed sizes depend strongly on frequency. As the frequency increases, the optimal seed sizes decrease. However, at high pressure amplitudes (>∼1 MPa), the optimal size appears to be dominated by the pressure amplitude, and at the highest pressure levels, the optimal seed size was approximately the same for all frequencies.

After obtaining the curves shown in Fig. 3, the next step was to find an approximate analytical expression relating the optimal seed size to the ultrasound pressure and frequency. This was done in two stages. First, given the flat slope followed by a linear decrease with pressure in the log domain, we hypothesized that the optimal seed size had a pressure dependence at each frequency of the form

$$R_{optimal}(P,f) = \frac{1}{\sqrt{G(f) + K \cdot P^2}} \tag{10}$$

where $G(f)$ is a function of frequency that is independent of pressure, K is an unknown constant, and P is the acoustic pressure amplitude. The constant, K, was then found by fitting the curve to

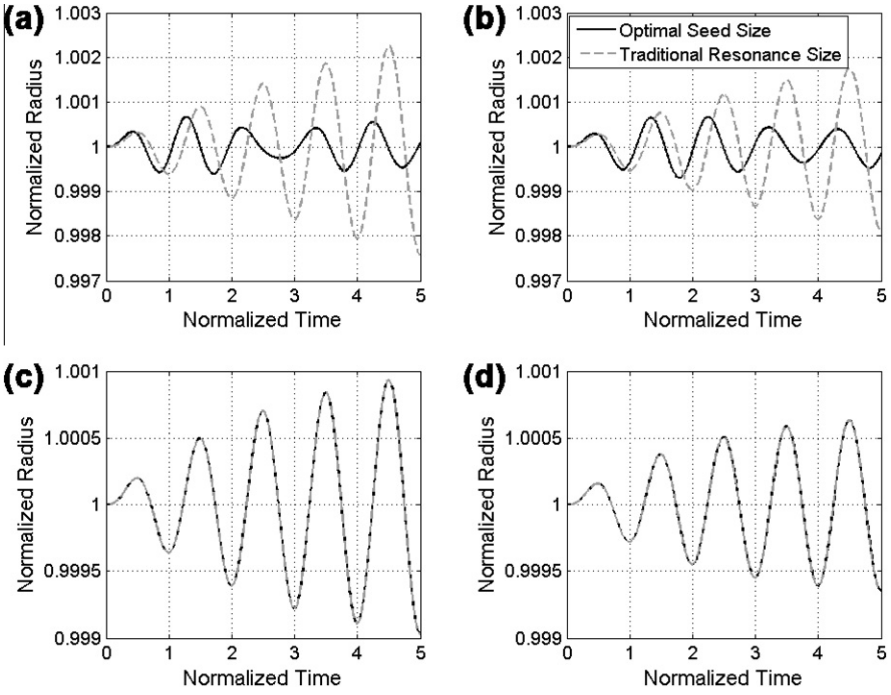

Fig. 2. The normalized radius (radius/initial radius) versus normalized time (time/period of acoustic wave) when the initial radius is our new optimal seed size (solid line) and the theoretical/traditional resonance size (dashed line) for a 100 Pa: (a) 0.5 MHz acoustical excitation of the bubble, (b) 1 MHz acoustical excitation of the bubble, (c) 3 MHz acoustical excitation of the bubble and (d) 5 MHz acoustical excitation of the bubble.

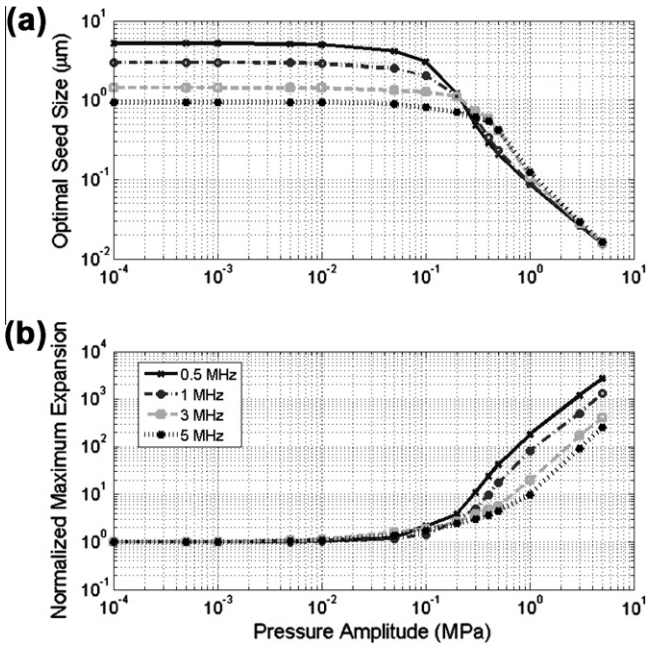

Fig. 3. (a) The optimal seed size resulting in the largest bubble expansion prior to the initial collapse and (b) the maximum expansion relative to the initial bubble size for pressure amplitudes from 100 Pa to 5 MPa for acoustic driving frequencies of 0.5, 1, 3, and 5 MHz.

the data set for each frequency independently (0.5, 1, 3, and 5 MHz) and then taking the mean value. For our data, K was found to be $16.5 \pm 4\ \mu m^{-2}\ MPa^{-2}$.

The next stage was to find the frequency dependence of $G(f)$ so that appropriate coefficients could be found. The values of $G(f)$ for our frequencies of 0.5, 1, 3, and 5 MHz are shown in Fig. 4 along with a quadratic fit. From this plot, it is clear that $G(f)$ is approximately a second order polynomial centered at the origin. Therefore, the optimal seed size in microns is approximately given by

$$R_{optimal}(\mu m) = \frac{1}{\sqrt{0.0327f^2 + 0.0679f + 16.5P^2}} \quad (11)$$

where f is frequency in MHz and P is the acoustic pressure amplitude in MPa. A comparison between the fit and the simulated data

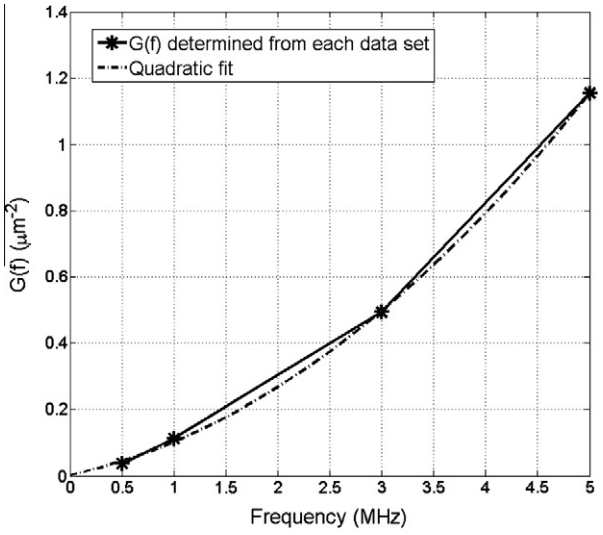

Fig. 4. The $G(f)$ values determined for frequencies of 0.5, 1, 3, and 5 MHz shown with fit by a second order polynomial.

is provided in Fig. 5. The fit is accurate to within 7% at low pressure amplitudes and overestimates the optimal size to within a factor of three at high pressure amplitudes (>1 MPa). The three constants found by the fit (i.e., $0.0327\ \mu m^{-2}\ MHz^{-2}$, $0.0679\ \mu m^{-2}\ MHz^{-1}$, and $16.5\ \mu m^{-2}\ MPa^{-2}$) likely depend on the properties of the bubble/fluid medium and should be investigated further in the future to obtain a better understanding of the physics behind the change in optimal seed size with pressure amplitude. It may also be possible in the future to obtain better analytical expressions by adding additional terms to (11), but this would complicate the expression making it less useful for 1st order calculations.

Before proceeding it is important to determine if an error on the order of a factor of three would be significant when using (11) as an approximate expression in therapeutic ultrasound applications. Therefore, the initial bubble size was varied about the optimal seed size found previously, and the maximum expansion relative to the initial size was determined for a 1 MHz 100 Pa (Fig. 6a) and for a 5 MPa (Fig. 6b) sinusoidal excitation. The peak shown in Fig. 6a corresponds to the theoretical resonance size while the peak in Fig. 6b corresponds to the optimal seed size that the search function revealed. Both the high and low amplitude excitations were included so that the dependence of the response on bubble size for both stable and inertial cavitation could be compared. The plots also show that as the pressure amplitude increases for the system the response peaks change shape. In the lower pressure amplitude case (100 Pa) shown in Fig. 5a the peak is narrow while in the high pressure amplitude case (5 MPa) the peak is much broader. This indicates that at higher pressure levels it is less critical to use bubbles at the optimal size to achieve results. Therefore, our approximate expression in (11) should be useful in a first order calculation.

3.2. Relationship between drop in optimal seed size and inertial cavitation

In order to determine if the drop in optimal seed size corresponds to the onset of inertial cavitation, the pressure threshold corresponding to the dramatic drop in optimal seed size and the dramatic increase in expansion were determined for each fre-

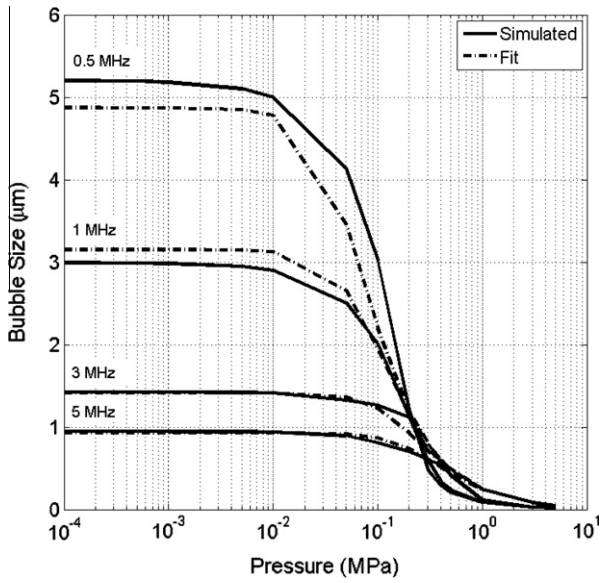

Fig. 5. The optimal bubble seed size plotted versus acoustical pressure for four different frequencies of 0.5, 1, 3, and 5 MHz. The solid curves are the optimal bubble sizes found by solving the complete Gilmore–Akulichev formulation for bubble dynamics [27,28]. The dashed curves represent a least squares fit to the data given by (11).

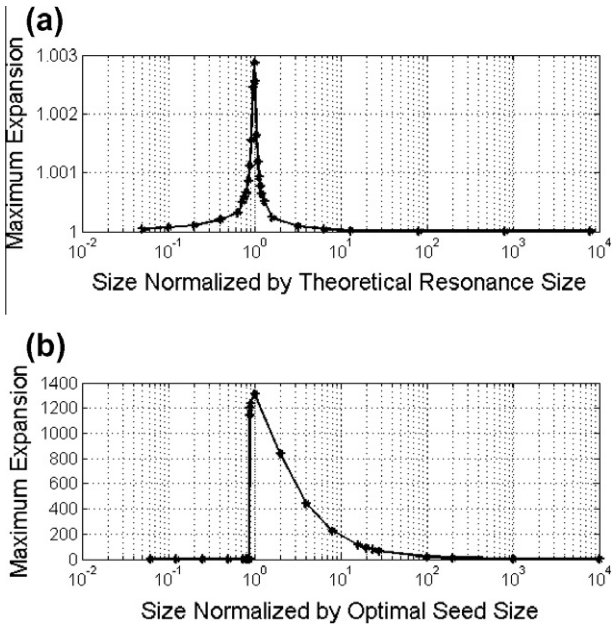

Fig. 6. Maximum expansion of the bubble relative to the initial size for: (a) a range of initial radii normalized with respect to the theoretical resonance size of 3.7 μm for an excitation frequency of 1 MHz and a pressure amplitude of 100 Pa and (b) a range of initial radii normalized with respect to the optimal seed size of 0.0155 μm for an excitation frequency of 1 MHz and a pressure amplitude of 5 MPa.

quency. The threshold values were determined by first fitting lines to the last three points in each plot for optimal seed size and also for maximum expansion. These three points corresponded to pressure amplitudes of 1, 3, and 5 MPa. The pressure threshold was then given as the pressure amplitude where this line intercepted the optimal seed size (dashed line) and the expansion sizes (solid line) at low excitation levels (i.e., 100 Pa) The pressure threshold values for all four frequencies for both resonance size and expansion are shown in Fig. 7. The threshold for the dramatic drop in resonance size is the same as the threshold for the dramatic increase in expansion indicating both effects have the same cause. When comparing the pressure thresholds from Fig. 7 to the maximum expansion curves in Fig. 3b, it is clear that the threshold pressures correspond to a maximum expansion of approximately 2 which has been used previously to quantify the onset of inertial cavitation [29]. Also, the pressure threshold corresponding to the dramatic drop in optimal seed size with pressure increases linearly with frequency, similar to what has been observed for inertial cavitation thresholds in the past [42]. Therefore, the dramatic drop in optimal seed size is likely due to the onset of inertial cavitation.

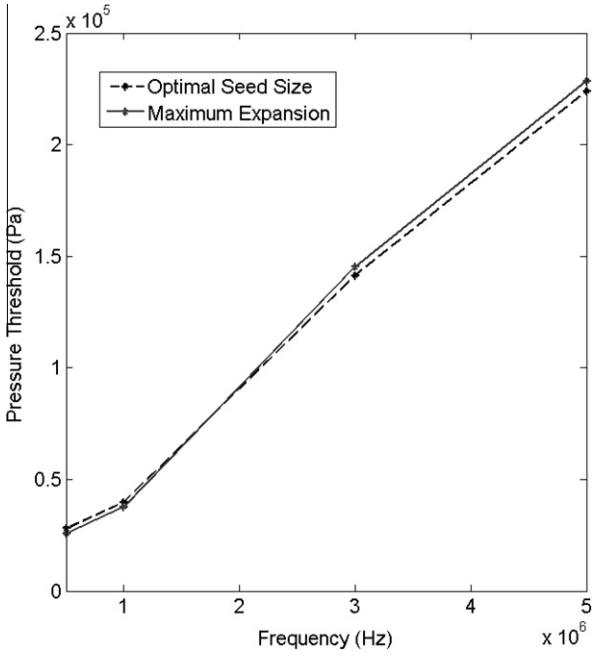

Fig. 7. The pressure threshold in Pascals for frequencies of 0.5 through 5 MHz for both the dramatic reduction in optimal seed size and the dramatic increase in maximum expansion.

4. Discussion/conclusions

The goal of our study was to develop an approximate expression relating the optimal initial "seed" size of the bubble to the ultrasound operating frequency and pressure of the ultrasound wave when inertial cavitation is expected which could be used for first order therapy planning and data analysis. A complete numerical study of inertial cavitation is often not feasible given the complications of bubble–bubble, bubble-tissue, and bubble cloud formation and destruction. However, an approximate expression that could provide information on relevant bubble sizes within an order of magnitude would help when initially planning procedures involving inertial cavitation. To this end, computer simulations were conducted and an approximate expression relating optimal bubble size to ultrasound pressure and frequency was determined.

The results of our computer simulations and derived expression indicate that as the pressure amplitude increases beyond some threshold, the optimal seed size of the bubble decreases dramatically eventually becoming independent of frequency. In addition, the maximum expansion of the bubble dramatically increases at the same threshold pressure. This pressure threshold is linearly dependent on frequency, correlates with a doubling of the bubble size, and is probably due to the onset of inertial cavitation. Also, our approximate expression agrees with our simulation results to within a factor of three at high pressure levels (>1 MPa). However, the response peak near the optimal seed size is much broader at higher pressure levels than has been observed for resonance size bubbles at lower pressure amplitudes. Therefore, having bubbles of the optimal size is not as critical when using bubbles in therapeutic applications and our approximate expression should give reasonable results (within an order of magnitude).

While our results did produce an approximate analytical expression for the optimal bubble size as a function of pressure and frequency for inertial cavitation applications, the accuracy is limited by several limitations of our technique. First, bubble to bubble interaction can impact resonance behavior [39,40] and in this study a single bubble was tested. In reality a large number of bubbles would be present. Many factors arise when dealing with numerous bubbles such as the spacing between the bubbles, bubble size, and asymmetric coupled collapse of the bubbles. Nonlinear propagation also affects the system and its unaccountability limits our model, and as noted, we used only linear acoustic waves to excite the bubbles. Nonlinear distortion of the wave would be present especially at the higher pressure amplitudes. Nonlinear distortion will result in an asymmetric waveform with the peak compressional pressure becoming significantly larger than the peak rarefractional pressure. At even higher pressures, shock waves can also appear in the waveform. Due to the nonlinear nature of bubble dynamics, nonlinear distortion/shock formation is likely to have an impact on the bubble response as well. Therefore, our approximate expression given in (11) is likely only valid to within an order of magnitude similar to (2) which is used when looking at stable cavitation applications.

Another potential short coming of the Gilmore–Akulichev formulation utilized in this paper was that it did not include heat or mass transfer. The neglection of heat transfer significantly simplifies the calculations and should only minimally impact the results given that the expansion of the bubble over the first cycle should not be significantly altered by heat conduction [27,28]. However, in order to estimate the impact on heat transfer, we changed the value of the polytropic exponent from 1.4 to 1.0 for the largest expansions found for our study. This changes the assumed process from adiabatic to isothermal. Previous studies have shown that the adiabatic assumption should underestimate the maximum radius of the bubble while an isothermal assumption should overestimate the maximum radius of the bubble [29]. By comparing the maximum radius from the two different approximations, we can approximate the error introduced by not accurately accounting for heat conduction. The cases compared were for the 5 MPa pressure amplitudes with initial bubble radii of .01538, 0.01549, 0.0160, and 0.0164 μm resulting in maximum expansions relative to the initial radii of 2701, 1313, 402.5, and 223.9 for driving frequencies of 0.5, 1, 3, and 5 MHz respectively. The new maximum expansions under isothermal conditions were found to be 3102, 1512, 462.8, and 259.5 respectively. Therefore, the percent difference between the adiabatic and isothermal cases relative to the average of the two cases was approximately 15% which is an acceptable difference given the other approximations made in this study.

Similarly, the impact of excluding mass transfer was assessed by comparing the bubble responses resulting in the maximum expansion for our study (5 MPa pressure amplitude with initial bubble radii of .01538, 0.01549, 0.0160, and 0.0164 μm resulting in maximum expansions relative to the initial radii of 2701, 1313, 402.5, and 223.9 for driving frequencies of 0.5, 1, 3, and 5 MHz respectively) to the bubble responses when using a different computer code [28] which included the Eller–Flynn formulation for diffusion [43]. Using this new code resulted in maximum expansions of 2679, 1305, 399, and 224 respectively. Therefore, the error introduced by neglecting mass transfer in our study was less than 1% indicating that mass transfer does not need to be included in future studies.

Acknowledgements

Special thanks to Charles Church (Associate Research Professor, University of Mississippi, Oxford, MS) for providing code that could be modified to calculate the bubble response. This work is supported by NSF Grant Award ECCS-0901942 "CAREER: Ultrasound Histotripsy System Development to Improve Cancer Treatment."

References

[1] W.W. Roberts, Focused ultrasound ablation of renal and prostate cancer: current technology and future directions, Urologic Oncology: Seminars and Original Investigations 23 (5) (2005) 367–371.
[2] F. Wu et al., Extracorporeal focused ultrasound surgery for treatment of human solid carcinomas: early Chinese clinical experience, Ultrasound in Medicine & Biology 30 (2) (2004) 245–260.
[3] J.L. Foley et al., Image-guided HIFU neurolysis of peripheral nerves to treat spasticity and pain, Ultrasound in Medicine & Biology 30 (9) (2004) 1199–1207.
[4] T. Christopher, HIFU focusing efficiency and a twin annular array source for prostate treatment, Ultrasonics, Ferroelectrics and Frequency Control, IEEE Transactions on 52 (9) (2005) 1523–1533.
[5] F.J. Fry, R.C. Eggleton, Ultrasonic device for human disease diagnosis and surgery, Technical Communication 78 (1972) 33–37.
[6] E.C. Everbach, C.W. Francis, Cavitational mechanisms in ultrasound-accelerated thrombolysis at 1 MHz, Ultrasound in Medicine & Biology 26 (7) (2000) 1153–1160.
[7] H.R. Guzman et al., Bioeffects caused by changes in acoustic cavitation bubble density and cell concentration: a unified explanation based on cell-to-bubble ratio and blast radius, Ultrasound in Medicine & Biology 29 (8) (2003) 1211–1222.
[8] J.C. Carmen et al., Treatment of biofilm infections on implants with low-frequency ultrasound and antibiotics, American Journal of Infection Control 33 (2) (2005) 78–82.
[9] S. Vaezy et al., Liver hemostasis using high-intensity focused ultrasound, Ultrasound in Medicine & Biology 23 (9) (1997) 1413–1420.
[10] S. Vaezy et al., Hemostasis of punctured blood vessels using high-intensity focused ultrasound, Ultrasound in Medicine & Biology 24 (6) (1998) 903–910.
[11] Z. Xu et al., Investigation of intensity thresholds for ultrasound tissue erosion, Ultrasound in Medicine & Biology 31 (12) (2005) 1673–1682.
[12] J.E. Parsons et al., Pulsed cavitational ultrasound therapy for controlled tissue homogenization, Ultrasound in Medicine & Biology 32 (1) (2006) 115–129.
[13] T.A. Bigelow et al., The destruction of *Escherichia coli* biofilms using high-intensity focused ultrasound, Ultrasound in Medicine & Biology 35 (6) (2009) 1026–1031.
[14] D.L. Miller, C. Dou, Induction of apoptosis in sonoporation and ultrasonic gene transfer, Ultrasound in Medicine & Biology 35 (1) (2009) 144–154.
[15] C.-Y. Lai et al., Quantitative relations of acoustic inertial cavitation with sonoporation and cell viability, Ultrasound in Medicine & Biology 32 (12) (2006) 1931–1941.
[16] T. Kodama et al., Transfection effect of microbubbles on cells in superposed ultrasound waves and behavior of cavitation bubble, Ultrasound in Medicine & Biology 32 (6) (2006) 905–914.
[17] Y. Manome et al., Insonation facilitates plasmid DNA transfection into the central nervous system and microbubbles enhance the effect, Ultrasound in Medicine & Biology 31 (5) (2005) 693–702.
[18] H. Pan et al., Study of sonoporation dynamics affected by ultrasound duty cycle, Ultrasound in Medicine & Biology 31 (6) (2005) 849–856.
[19] V.G. Zarnitsyn, M.R. Prausnitz, Physical parameters influencing optimization of ultrasound-mediated DNA transfection, Ultrasound in Medicine & Biology 30 (4) (2004) 527–538.
[20] C.A. MacDonald et al., A numerical investigation of the resonance of gas-filled microbubbles: resonance dependence on acoustic pressure amplitude, Ultrasonics 43 (2) (2004) 113–122.
[21] K.E. Morgan et al., Experimental and theoretical evaluation of microbubble behavior: effect of transmitted phase and bubble size, Ultrasonics, Ferroelectrics and Frequency Control, IEEE Transactions on 47 (6) (2000) 1494–1509.
[22] W. Lauterborn, Numerical investigation of nonlinear oscillations of gas bubbles in liquids, The Journal of the Acoustical Society of America 59 (2) (1976) 283–293.
[23] R.Y. Nishi, Scattering and absorption of sound waves by a gas bubble in a viscous liquid, Acustica 33 (2) (1975) 65–74.
[24] T.G. Leighton, The Acoustic Bubble, Academic Press Inc., San Diego, 1994. p. 139.
[25] M. Minnaert, On musical air-bubbles and the sounds of running water, Philosophical Magazine Series 7 16 (104) (1933) 235–248.
[26] A.Y. Ammi et al., Ultrasonic contrast agent shell rupture detected by inertial cavitation and rebound signals, Ultrasonics, Ferroelectrics and Frequency Control, IEEE Transactions on 53 (1) (2006) 126–136.
[27] C.C. Church, A theoretical study of cavitation generated by an extracorporeal shock wave lithotripter, The Journal of the Acoustical Society of America 86 (1) (1989) 215–227.
[28] C.C. Church, Prediction of rectified diffusion during nonlinear bubble pulsations at biomedical frequencies, The Journal of the Acoustical Society of America 83 (6) (1988) 2210–2217.
[29] H.G. Flynn, C.C. Church, Transient pulsations of small gas bubbles in water, The Journal of the Acoustical Society of America 84 (3) (1988) 985–998.
[30] F. Chavrier et al., Modeling of high-intensity focused ultrasound-induced lesions in the presence of cavitation bubbles, The Journal of the Acoustical Society of America 108 (1) (2000) 432–440.
[31] D. Chatterjee, K. Sarkar, A Newtonian rheological model for the interface of microbubble contrast agents, Ultrasound in Medicine & Biology 29 (12) (2003) 1749–1757.
[32] J.C. Machado, J.S. Valente, Ultrasonic scattering cross sections of shell-encapsulated gas bubbles immersed in a viscoelastic liquid: first and second harmonics, Ultrasonics 41 (8) (2003) 605–613.
[33] J. Jimenez-Fernandez, A. Crespo, Bubble oscillation and inertial cavitation in viscoelastic fluids, Ultrasonics 43 (8) (2005) 643–651.
[34] S.M. Gracewski, H. Miao, D. Dalecki, Ultrasonic excitation of a bubble near a rigid or deformable sphere: implications for ultrasonically induced hemolysis, The Journal of the Acoustical Society of America 117 (3) (2005) 1440–1447.
[35] K. Chetty, J.V. Hajnal, R.J. Eckersley, Investigating the nonlinear microbubble response to chirp encoded, multipulse sequences, Ultrasound in Medicine & Biology 32 (12) (2006) 1887–1895.
[36] E. Kimmel et al., Subharmonic response of encapsulated microbubbles: conditions for existence and amplification, Ultrasound in Medicine & Biology 33 (11) (2007) 1767–1776.
[37] R.T. Beyer, Nonlinear Acoustics, Acoustical Society of America, Woodbury, NY, 1997. pp. 269–283.
[38] T.G. Leighton, The Acoustic Bubble, Academic Press Inc., San Diego, 1994. pp. 306–308.
[39] N.C. Skaropoulos, H.D. Yagridou, D.P. Chrissoulidis, Interactive resonant scattering by a cluster of air bubbles in water, The Journal of the Acoustical Society of America 113 (6) (2003) 3001–3011.
[40] J.S. Allen et al., Effect of coupled oscillations on microbubble behavior, The Journal of the Acoustical Society of America 114 (3) (2003) 1678–1690.

[41] G.J. Lastman, R.A. Wentzell, Comparison of five models of spherical bubble response in an inviscid compressible liquid, The Journal of the Acoustical Society of America 69 (3) (1981) 638–642.
[42] C.K. Holland, R.E. Apfel, An improved theory for the prediction of microcavitation thresholds, Ultrasonics, Ferroelectrics and Frequency Control, IEEE Transactions on 36 (2) (1989) 204–208.
[43] A. Eller, H.G. Flynn, Rectified diffusion during nonlinear pulsations of cavitation bubbles, The Journal of the Acoustical Society of America 37 (3) (1965) 493–503.